Prohibitin promotes apoptosis of promyelocytic leukemia induced by arsenic sulfide

PENGCHENG HE[1*], YANFENG LIU[1*], JUN QI[2], HUACHAO ZHU[1], YUAN WANG[1], JING ZHAO[1], XIAOYAN CHENG[1], CHEN WANG[1,3] and MEI ZHANG[1]

[1]Department of Hematology, The First Affiliated Hospital, Xi'an Jiaotong University, Xi'an, Shaanxi; [2]Institute of Xi'an Blood Bank, Shaanxi Blood Center, Xi'an, Shaanxi, P.R. China; [3]Pathology and Laboratory Medicine, Mount Sinai Hospital, Toronto University, Toronto, ON, Canada

Received August 8, 2015; Accepted September 22, 2015

DOI: 10.3892/ijo.2015.3217

Abstract. Arsenic sulfide (As_4S_4), an oral form of arsenic agent, has been shown to have similar efficacy and safety to intravenous arsenic trioxide in the treatment of acute promyelocytic leukemia (APL). The aim of the present study was to identify proteins modulated by As_4S_4 and to determine their involvement in the apoptotic pathway. We used comparative proteomic analysis to screen and identify the proteins that were differentially expressed with As_4S_4 treatment. Prohibitin (PHB) was selected for its diverse role and its increased expression in the cells treated with As_4S_4. To examine whether PHB play a functional role, two clones of PHB-knockdown and PHB-overexpression were generated by transfection of NB4-R1 with vectors containing PHB gene sequences. In comparison with parental NB4-R1 cells, PHB overexpression showed an increase in baseline apoptosis and an enhanced response in As_4S_4-induced apoptosis. PML-RARα fusion protein was found to be reduced with PHB-overexpression, and following As_4S_4 treatment, a greater reduction of promyelocytic leukemia-retinoic acid receptor-α (PML-RARα) fusion protein was seen in PHB-overexpression than that in parental cells. Consistently, PHB knockdown presented with a significant reduction in As_4S_4-induced apoptosis and a lesser degree of PML-RARα degradation. The results indicate the antitumor activity of PHB in promoting apoptosis of APL cells.

Correspondence to: Professor Mei Zhang, Department of Hematology, The First Affiliated Hospital of Xi'an Jiaotong University, 277 Yanta West Road, Xi'an, Shaanxi 710061, P.R. China
E-mail: zhangmei_xjtu@hotmail.com

*Contributed equally

Abbreviations: As_4S_4, arsenic sulfide; APL, acute promyelocytic leukemia; PHB, prohibitin; ATRA, all-*trans* retinoic acid; PML-RARα, promyelocytic leukemia-retinoic acid receptor-α

Key words: prohibitin, apoptosis, acute promyelocytic leukemia, arsenic sulfide, all-*trans* retinoic acid

Introduction

Acute promyelocytic leukemia (APL) is characterized by specific chromosomal translocations, typically t(15;17), which results in the formation of the promyelocytic leukemia-retinoic acid receptor-α (PML-RARα) fusion gene (1,2). PML-RARα fusion protein forms homo/heterodimers that sequestrate RXR and/or PML proteins in a large protein complex and disrupt the retinoic acid (RA) signal pathway. This specific oncogenic lesion determines characteristic cell morphology and clinical presentations, and it also determines the unique response to the treatment with all-*trans* retinoic acid (ATRA) or arsenic agents (3,4). Both drugs have been demonstrated to target the PML/RARα oncoprotein for proteasome-mediated degradation. Clinically, ATRA induces complete remissions in ~90% of newly diagnosed APL, but many patients eventually experience a relapse and develop ATRA-resistance (5,6). Arsenic trioxide is also shown to be effective in the treatment of APL, especially in relapsed APL with ATRA-resistance (7,8).

Arsenic trioxide has dual effects of inducing differentiation and apoptosis of APL cells. However, there are issues of availability and cost of arsenic trioxide that limit its general applications. The development of oral form of arsenic drug may promote its applications in APL. Arsenic sulfide (As_4S_4), also known as realgar, is an oral arsenic formulation. This oral arsenic drug has been shown to have similar effect and safety to intravenous arsenic trioxide in the treatment of newly diagnosed and relapsed/refractory APL or ATRA-resistance (9). The therapeutic action of As_4S_4 is closely associated with its function of inducing apoptosis. Although it is known that As_4S_4 induces cell apoptosis through degrading PML-RARα fusion protein (10), the definitive molecular mechanisms of action of As_4S_4 remain unclear and require further investigations.

In the present study, we used a comparative proteomic approach to screen and identify proteins that are differentially expressed in APL cells induced by As_4S_4. By using two-dimensional gel electrophoresis (2-DE) followed by a matrix-assisted laser desorption/ionization-time-of-flight mass spectrometry (MALDI-TOF MS) analysis, we identified prohibitin (PHB)

among the differentially expressed proteins. PHB was significantly upregulated in ATRA-resistance APL cells (NB4-R1) by As_4S_4 treatment. Further studies of PHB-knockdown and PHB-overexpression indicate a functional role of PHB in As_4S_4-induced apoptosis of NB4-R1 cells.

Materials and methods

Cell culture. The ATRA-resistance human APL cell line (NB4-R1), received from Shanghai Institute of Hematology, (Shanghai, China) was maintained in cultures with RPMI-1640 medium (Gibco-BRL, Carlsbad, CA, USA) supplemented with 10% heated-inactivated fetal bovine serum (FBS) at 37˚C in a humidified incubator containing 5% CO_2.

Cell viability assay. Cytotoxicity of As_4S_4 (Xi'an Traditional Chinese Drug Company, Xi'an, China) was assessed by using MTT assay (Sigma, St. Louis, MO, USA) (11). The absorbance was measured at 570 nm using a universal microplate reader (Model ELx800; BioTek Instruments, Inc., Winooski, VT, USA). Experiments were performed in triplicate.

Apoptosis evaluation. Transmission electron microscopy (TEM) and flow cytometric analysis (FCM) were performed to evaluate cell apoptosis. After the various treatments, the cell samples were examined under a JEM-100SX electron microscope (JEOL, Ltd., Tokyo, Japan) and were analyzed in a FACSCalibur flow cytometer (Becton-Dickinson, San Jose, CA, USA) and CellQuest software, respectively. All experiments were performed in triplicate.

2-DE and image analysis. Total cellular proteins were prepared from NB4-R1 cells before and after As_4S_4 treatment. Protein extraction was performed by sonication in a sample buffer (SB) containing 40 mM Tris base, 8 M urea, 2 M thiourea, 4% (w/v) CHAPS, 1% (w/v) dithiothreitol (DTT), 1 mM EDTA and protease inhibitor cocktail (Roche Diagnostics Ltd., Mannheim, Germany). For nuclei enrichment cells were dissolved in 200 μl of lysis buffer [10 mM HEPES, 1.5 mM $MgCl_2$, 10 mM KCl, 0.5 mM DTT, in the presence of protease inhibitor cocktail (Sigma), 20 ng/μl DNase and 20 ng/μl RNase] and incubated on ice for 30 min. After incubation, NP-40 (Roche) was added at final concentration of 0.5% (v/v). After centrifugation at 14,000 rpm for 30 min at 4˚C, the supernatant was used for analysis with the protein concentration determined by the Bradford method with a commercial Bradford reagent (Bio-Rad Laboratories, Hercules, CA, USA) (12).

2-DE was performed as described by Görg *et al* (13). Briefly, 140 μg of protein (for silver nitrate staining gels) or 1.4 mg of protein (for coomassie brilliant blue staining gels) was diluted to 350 μl with rehydration solution and applied onto 18 cm (pH 3-10) not linear immobilized pH gradient dry strip (Amersham Pharmacia Biotech, Uppsala, Sweden). After the strips were rehydrated, isoelectric focusing was performed in the IPGphor system (Amersham Pharmacia Biotech) according to the manufacturer's protocol (14). The strips were equilibrated for 15 min in a solution containing 6 M urea, 2% (w/v) SDS, 20 mM DTT, 30% (w/v) glycerol and 50 mM Tris-HCl (pH 8.8). A second equilibration was also carried out for 15 min in the same solution except for DTT replaced by 100 mM iodoacetamide. The second dimension was performed on 13% SDS-polyacrylamide gradient gels using the PROTEAN XI Cell (Bio-Rad Laboratories) at 20 mA/gel for 40 min.

Silver nitrate staining according to the protocol of Lelong *et al* (15), and coomassie brilliant blue R-250 (0.05% brilliant blue) was used for the analytical and preparative gels. The 2-DE images were acquired using Image scanner (Amersham Pharmacia Biotech). Gel images were analyzed by the ImageMaster 2D Platinum software (Amersham Pharmacia Biotech). Spot detection and normalization were performed by the automated software tools.

MALDI-TOF MS and MALDI-TOF MS/MS analysis. Differentially expressed spots were manually excised from 2-DE gels. Gel pieces were destained and digestion. In-gel digestion was done according to the protocol of Granvogl *et al* (16).

MALDI-TOFMS analysis was performed on a Bruker REFLEX III MALDI-TOF-MS (Bruker-Franzen, Bremen, Germany). Peptides were desalted by C18 ZipTips (Millipore, Billerica, MA, USA) and co-crystallized with a solution of 0.5 mg/ml α-cyano-4-hydroxycinnamic acid dissolved in acetonitrile/0.1% (v/v) trifluoroacetic acid (TFA) in H_2O (1:1) pre-spotted with a thin layer of 10 mg/ml α-cyano-4-hydroxycinnamic acid dissolved in ethanol/acetonitrile/0.1% (v/v) TFA in H_2O (49.5:49.5:1). Monoisotopic peptide masses were used to search the database, allowing a peptide mass accuracy of 0.3 Da and one partial cleavage. The proteins were identified by peptide mass fingerprinting (PMF) searching, against the Swiss-Prot databases and NCBI databases, using the search program Mascot (http://www.matrixscience.com).

The protein spots which were not identified by MALDI-TOF-MS were analyzed by MALDI-TOF MS/MS. MALDI-TOF MS/MS analysis was performed in LIFT mode. Precursor ions were selected manually. MS/MS spectra were acquired with a minimum of 4000 and a maximum of 8000 laser shots using the instrument calibration file. The precursor mass window was set automatically after the precursor ion selection. Spectra baseline subtraction, smoothing (Savitsky-Golay) and centroiding was performed by FlexAnalysis software (version 3.0; Bruker Daltonik GmbH, Bremen, Germany).

Western blot analysis. Cell protein extracts were prepared following standard procedures. The protein samples (~20 mg) were separated by SDS-PAGE. After SDS-PAGE, proteins were transferred to nitrocellulose membranes (Invitrogen, Carlsbad, CA, USA). The filters were washed, blocked with 5% bovine serum albumin (BSA) in Tris-buffered saline (25 mM Tris, pH 7.4, 136 mM NaCl, 2.6 mM KCl and 0.5% Tween-20) for 1 h, and incubated overnight with mouse anti-PHB antibody diluted to 1:700 (Abcam, Cambridge, MA, USA) at room temperature. After washing three times with TBST buffer, the membranes were incubated with the secondary HRP-conjugated goat anti-mouse IgG Ab (Santa Cruz Biotechnology, Santa Cruz, CA, USA) at 1:10,000 dilution. Mouse anti-GAPDH antibody (Santa Cruz Biotechnology) was used to ensure equal loading of samples.

Quantitative real-time PCR (qRT-PCR). The total RNA from cells was isolated with TRIzol (Life Technologies, Rockvile, MD, USA) and reverse-transcribed to cDNA by using the PrimeScript™ RT reagent kit (Takara Bio, Dalian, China). The cDNA was studied using a CFX96 real-time PCR system (Bio-Rad Laboratories) with SYBR-Green PCR Master Mix (Takara) to determine the transcriptional expression of PHB gene. PCR products were electrophoresed on 1.5% agarose gels. The GAPDH was used for normalization, relative gene expression was calculated by the $2^{-\Delta\Delta Ct}$ method.

Knockdown and overexpressing of PHB. Lentiviral vector-mediated shRNA targeting human PHB mRNA (named pGCSIL-GFP-PHB) was previously described (17). The target sequences on the human PHB gene (GeneBank accession number NM_002634) for RNAi were designed using an internet application system as follows: 5'-GAGTTCACAGA AGCGGTGGAA3'. A shRNA which had no significant homology to any known human gene (5'-TTCTCCGAACGT GTCACGT-3') was used as a negative control. Oligonucleotides were ligated into the *Age*I and *Eco*RI sites of pGCSIL-GFP vector (BD Biosciences, San Jose, CA, USA) to generate a pGCSIL-GFP-PHB, which was then transformed into *E. coli*. Positive recombinant clones were selected by PCR (upstream primer: 5'-CCTATTTCCCATGATTCCTTCATA-3'; downstream primer: 5'-GTAATACGGTTATCCACGCG-3') and DNA sequencing. The recombinant lentivirus vector was produced by co-transfecting 293T cells with the lentivirus expression plasmid and packaging plasmids (pHelper 1.0 and pHelper 2.0) with Lipofectamine 2000 (Invitrogen). Infectious lentivirus vector was harvested at 48 h post-transfection and then concentrated. The infectious titer was determined by the GFP-tagged positive rate in 293T cells. NB4-R1 cells were cultured at a density of $6x10^5$/well in 6-well plates and infected with lentivirus in RPMI-1640 media containing 10% FBS and 8 μg/ml of polybrene (Sigma), at the multiplicity of infection (MOI) 20, according to the pre-experimental results. After 48 h of culture, the transduction efficiency was ascertained on the basis of GFP expression under a fluorescence microscope. The knockdown efficiency of PHB was analyzed by real-time quantitative PCR and western blot analysis. NB4-R1 cells transfected with vector containing pGCSIL-GFP-PHB were designated as PHB-knockdown (KD).

The PHB gene overexpression vector (named pEGFP-N1-3FLAG-PHB) was also established. Briefly, the cDNA fragment of PHB was amplified using a PCR-based approach (upstream primer: 5'-CCGCTCGAGATGGCTGCCAAAGT GTTTG; downstream primer: 5'-GGGGTACCGTCTGGGG CAGCTGGAGGAG) from a cDNA library. The PCR fragment of confirmed sequences was ligated into the *Xho*I and *Kpn*I sites of overexpression vector pEGFP-N1-3FLAG (BD Biosciences). The resultant construct, pEGFP-N1-3FLAG-PHB, was transformed into *E. coli*. Positive recombinant clones were selected by PCR and DNA sequencing (upstream primer: 5'-CGCAAATGGGCGGTAGGCGTG-3'; downstream primer: 5'-CGTCGCCGTCCAGCTCGACCAG-3'). The expression of PHB was analyzed by real-time quantitative PCR and western blot analysis. The NB4-R1 cell clone transfected with the vector containing pEGFP-N1-3FLAG-PHB were designated as PHB-overexpression (OE).

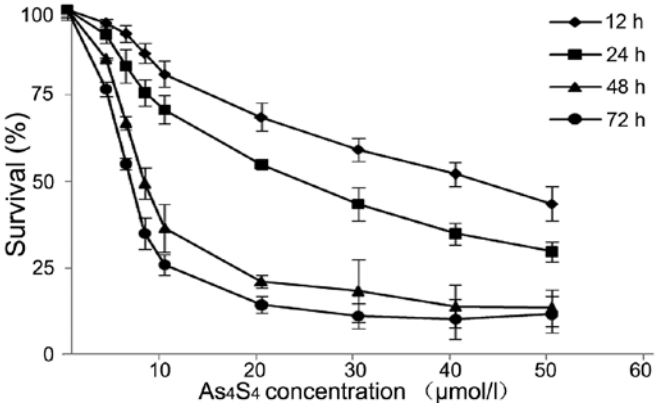

Figure 1. Dose- and time-dependent inhibition of NB4-R1 cells as determined by the MTT assay. The results are expressed as a percentage of viable cells compared with control cells. Each value represents the mean ± SD of triplicate experiments.

Statistical analysis. The results are expressed as mean ± standard deviation values of three experiments performed in duplicate. Statistical analysis was carried out by one-way analysis of variance. Newman-Keuls test was used for the identification of statistically significant differences in spot volume percentage among different samples. Differences were considered statistically significant when $P<0.05$.

Results

As_4S_4 inhibits the growth of ATRA-resistant NB4-R1 cells. We started with MTT assay to evaluate the cytotoxicity of As_4S_4 on ATRA-resistant NB4-R1 cells. The results demonstrated that As_4S_4 inhibited the growth of NB4-R1 cells in a dose- and time-dependent manner (Fig. 1). The IC_{50} values of As_4S_4 were determined at 43.04±0.11 μM for 12 h, 25.07±0.27 μM for 24 h, 9.70±0.13 μM for 48 h and 6.38±0.09 μM for 72 h in culture. The concentration of 25 μM, the IC_{50} of As_4S_4 at 24 h, was chosen for subsequent experiments.

As_4S_4 induces apoptosis of NB4-R1 cells. As_4S_4-induced apoptosis was assessed by using TEM and FCM analysis. The NB4-R1 cells treated with As_4S_4 showed morphological features of cytoplasmic vacuolization, chromatin condensation, nuclear fragmentation and formation of apoptotic bodies (Fig. 2A). The apoptotic cells were quantified by FCM assay for Annexin V^+ cells. The percentage of apoptotic cells was significantly increased with As_4S_4 treatment for 24 and 48 h (Fig. 2B).

PHB is an upregulated protein induced by As_4S_4. We next used proteomic approaches to screen and identify proteins that were differentially expressed following As_4S_4 treatment. The comparison of 2-DE protein profiles of NB4-R1 cells at 0 h with that at 24 and 48 h As_4S_4 treatment were performed, and 22 protein spots with at least a 2-fold increase or decrease in density were selected for further analysis (Fig. 3A and B).

These spots were cut out, followed by in-gel trypsin digestion and MALDI-TOF MS analysis. The protein spots which were not identified by MALDI-TOF-MS were further

Table I. Identification of differentially expressed protein spots by MALDI-TOF-MS and MALDI-TOF-MS/MS.

Spot	Protein name	NCBInr ID no.	Function classification	Mr (Da)		pI		Peptides (MALDI/MS)		Sequence coverage (%)	Protein expression[b] R24/R48
				Theor.	Observ.	Theor.	Observ.	Match	Total		
D1	Poly C binding protein 1 (PCBP1)	gil6754994	Regulates gene expression	37474	43062	6.66	7.83	17	28	52	0.57/0.19
D2	Acidic leucine-rich nuclear phosphoprotein 32 family member A (ANP32A)	gil5453880	Cell proliferation, differentiation, apoptosis	28568	30123	3.99	3.88	8	14	31	0.70/0.42
D3[a]	SET/protein phosphatase 2A inhibitor (SET/I2PP2A)	gil170763500	Multitasking protein	33469	41249	4.23	4.01	7	13	27	0.34/0.10
D4	Eukaryotic translation initiation factor 4H isoform 1 (eIF4H-1)	gil11559923	Protein synthesis	27368	32661	6.67	7.16	14	29	48	0.64/0.20
D5	60S acidic ribosomal protein P2 (RPP2)	gil4506671	Protein synthesis	11658	16831	4.42	4.13	7	20	77	0.40/0.30
U1	High mobility group protein B1 (HMGB1)	gil4504425	Signal transduction	24878	29744	5.62	6.88	11	20	48	4.58/2.95
U2	Transgelin-2 (TAGLN2)	gil4507357	Not be determined	22377	20417	8.41	5.58	15	19	56	2.50/6.07
U3	Eukaryotic translation initiation factor5A) (eIF5A-1	gil183448388	Protein synthesis, cellular growth, differentiation and proliferation	16821	16949	5.08	7.37	9	31	52	2.46/10.14
U4	Transcription factor(TF)	gil388307	Transcription	20700	22567	6.28	5.49	2	43	12	6.18/19.98
U5	α-tubulin	gil37492	Cellular motility and transportation	50126	22567	5.02	5.49	3	26	9	6.18/19.98
U6	Histone H2B type 1-M (H2B1M)	gil4504263	Transcription, DNA repair	13981	16949	10.31	7.37	12	31	67	2.12/15.87
U7	Rho GDP dissociation inhibitor β 2 (RhoGDI2)	gil56676393	Signal transduction and regulates Rho GTPases	22974	24685	5.10	7.01	8	33	54	5.31/16.83
U8	Prohibitin (PHB)	gil4505773	Cell proliferation, tumor suppressor	29786	31560	5.57	5.37	13	14	61	2.18/3.68
U9	Ribosomal phosphoprotein P0 (RPP0)	gil4506667	Protein synthesis and apoptosis	34252	39054	5.71	6.27	14	19	46	16.16/22.4
U10	Heat shock 27 kDa protein (HSP27)	gil4504517	Stress resistance	22768	28891	5.98	6.34	11	18	46	2.77/1.79
U11	Elongation factor 1-β (EF-1-β)	gil18203449	Protein synthesis	24748	32071	4.50	4.38	6	13	37	1.53/2.84
U12	Keratin-2	gil47132620	Proliferation and keratinization	65393	18903	8.07	6.21	11	38	25	4.23/14.82
U13	ERP29	gil5803013	Protein processing	28975	31332	6.77	5.89	12	28	42	1.30/5.06
U14	β-actin (ACTB)	gil4501885	Cellular motility	41710	14843	5.29	8.26	10	20	23	1.90/13.48
U15	GTPase-activating protein	gil62911375	Increase GTP hydrolysis	23439	27647	5.21	5.25	6	17	30	1.70/3.27
U16[a]	Neuropolypeptide h3	gil913159	Serine protease inhibitor	20913	66684	7.42	5.88	-	-	31	0.95/3.18
U17	Proteasome β 4 subunit (PSMB4)	gil22538467	Proteolysis	29185	28177	5.72	5.56	13	25	35	1.32/3.42

D, downregulation; U, upregulation; pI, isoelectric point; Mr, molecular weight. [a]The spot is identified by MALDI-TOF-MS and MALDI-TOF-MS/MS; [b]As_4S_4-treated (R24 and R48) divided by untreated (R0); all values are statistically significant, $P<0.05$.

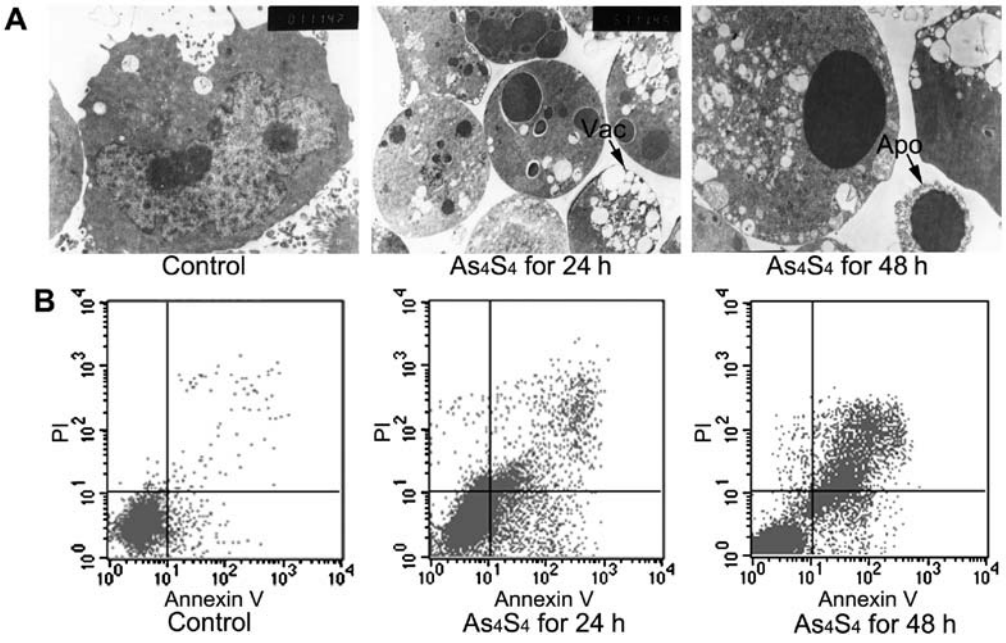

Figure 2. Evaluation of apoptosis of NB4-R1 cells induced by As_4S_4. (A) Ultrastructural changes. Cells treated with As_4S_4 for 24 h showed cytoplasmic vacuolization (Vac) and chromatin condensation, and cells treated with As_4S_4 for 48 h showed nuclear fragmentation and formation of apoptotic bodies (Apo). Original magnification, x5000. (B) Flow cytometric analysis of NB4-R1 cells apoptosis induced by As_4S_4. The percentage of apoptotic cells (Annexin V^+) was 2.7, 33.4 and 44.5% in control, As_4S_4 24 and 48 h, respectively.

analyzed by MALDI-TOF MS/MS. PMF and peptide amino acid sequence were analyzed for protein identification using the Mascot search program. Fig. 3C showed the PMF of spot U8 analyzed by MALDI-TOF-MS. spot U8 was identified as prohibitin (PHB) and the corresponding protein sequence is shown in Fig. 3D. The annotation of the 22 identified proteins is shown in Table I.

PHB was identified from the spot U8, which was upregulated induced by As_4S_4. The increase in PHB protein was confirmed by western blot analysis. As shown in Fig. 3E, there was a 2.0- and 3.9-fold increase in PHB protein with As_4S_4 for 24 and 48 h, respectively. At mRNA level, PHB expression was increased by 1.8- and 3.2-fold with As_4S_4 for 24 and 48 h, respectively (Fig. 3F). The results indicate an upregulation of PHB gene expression at both mRNA and protein levels.

Generation of PHB-overexpression and PHB-knockdown NB4-R1 cells. To investigate whether PHB plays a functional role in NB4-R1 cell apoptosis, we used the PHB gene overexpressing vector (pEGFP-N1-3FLAG-PHB) to generate PHB-overexpression NB4-R1 cells (OE group). The PHB-overexpression efficiency was then validated by qRT-PCR and western blot analysis, respectively. Our results showed that PHB expression in OE group was increased by 67.8% at mRNA level and 45.8% at protein level (Fig. 4A and B). Similarly, the RNA interference vector (pGCSIL-GFP-PHB) of PHB gene was used to generate PHB-knockdown NB4-R1 cells (KD group). Our results showed that PHB expression was reduced by 83.5% at mRNA level and 89.7% at protein level, respectively (Fig. 4C and D).

PHB-overexpression promotes NB4-R1 apoptosis and PML-RARα fusion protein degradation. Our results showed after 48 h of transfection, the percentages of apoptotic cells in OE group was increased by 3.8-fold in comparison with the parental NB4-R1 cells (26.73±6.53 vs. 7.11±1.02%, P<0.01) (Fig. 5A), and the PML-RARα fusion protein was reduced by 1.5-fold in comparison with the control (34.21±3.81 vs. 51.31±8.55%, P<0.01) (Fig. 5B).

The response of the OE cells to As_4S_4 was evaluated in comparison with parental NB4-R1 cells. OE cells showed an increase in As_4S_4-induced apoptosis. With As_4S_4 at the concentration of 25 μM for 48 h, the apoptotic cells in NB4-R1 and OE cells were 48.33±9.84 and 58.71±11.74%, respectively (Fig. 5A). PML-RARα fusion protein was assessed by western blot analysis, and the results showed that As_4S_4 treatment led to greater reduction of PML-RARα protein in OE cells than that in NB4-R1 cells. In comparison with untreated NB4-R1 cells, As_4S_4 treatment reduced PML-RARα protein by 51.0 and 76.9% in NB4-R1 and OE cells, respectively (the grayscale ratios of PML-RARα/GAPDH: 25.14±2.87 and 11.86±2.99%, P<0.05) (Fig. 5B).

PHB-knockdown reduces As_4S_4-induced apoptosis and degradation of PML-RARα protein. PHB-knockdown NB4-R1 cells (KD) was evaluated in comparison with parental NB4-R1 cells. With no As_4S_4 treatment, there was no significant difference in the baseline apoptotic cells between KD and NB4-R1 cells. Similarly, no significant difference was seen between KD and the NB4-R1 in the expression of PML-RARα fusion proteins, as determined by PML-RARα/GAPDH (53.16±7.83 vs. 49.78±1.89%) (Fig. 6A and B).

The KD cells were then used to examine its response to As_4S_4 treatment. As_4S_4-induced apoptosis was evaluated with As_4S_4 at the concentration of 25 μM for 48 h. In comparison with parental NB4-R1 cells, the KD showed a lesser degree of cellular apoptosis. The percentages of apoptotic cells in NB4-R1 and KD were determined to be 45.17±5.43 and

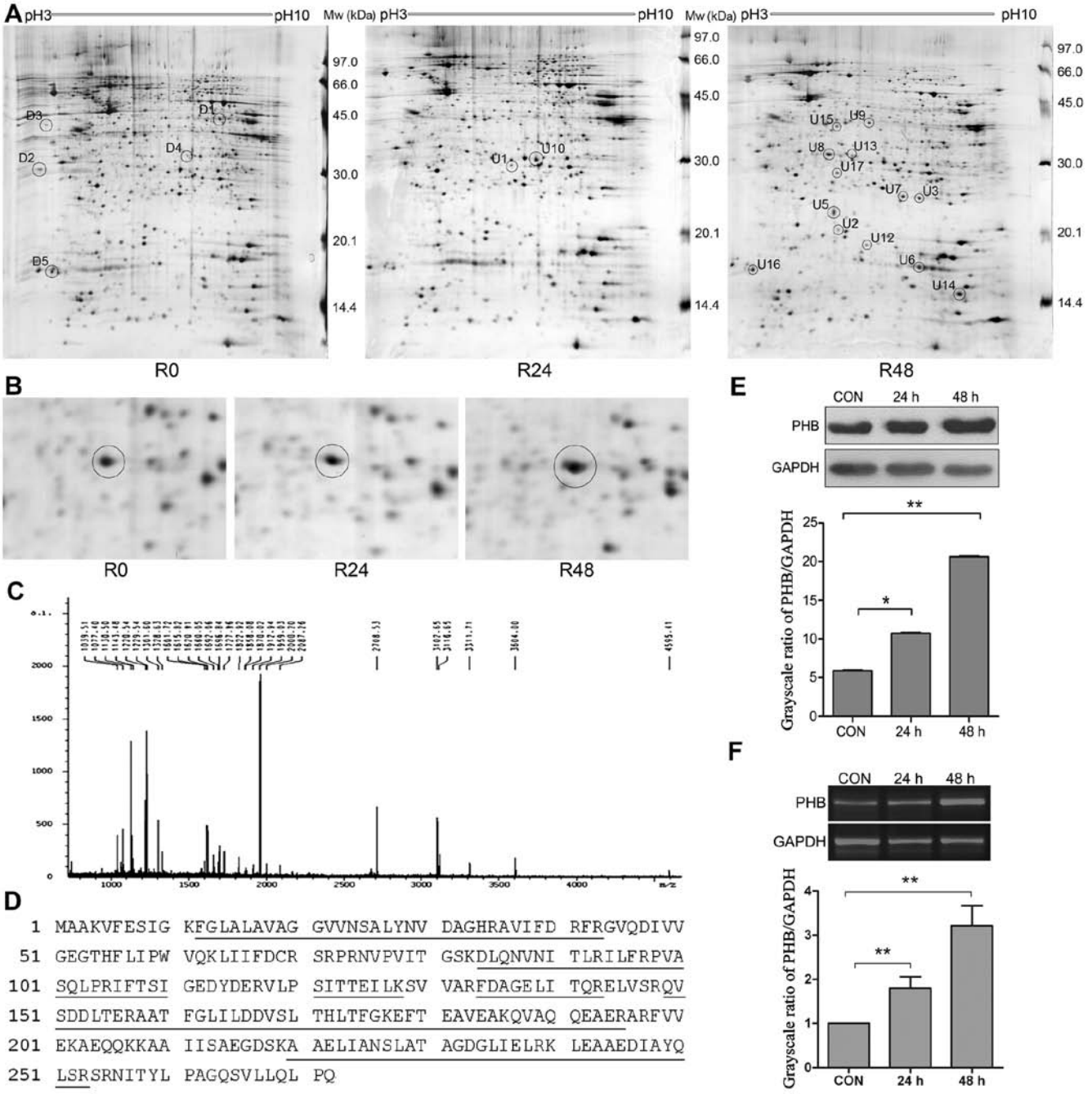

Figure 3. Selection and identification of upregulated PHB in NB4-R1 cells induced by As_4S_4. (A) Representative silver-stained 2-DE maps of NB4-R1 cells untreated (R0), treated with As_4S_4 for 24 h (R24) and 48 h (R48). Circles indicate the protein spots identified by MS or MS/MS. (B) The amplified image of differential expression protein spot U8 in R0, R24 and R48. Spot U8 showed increase in intensity at R24 and R48. (C) MALDI-TOF-MS analysis of differential protein spot U8. Spot U8 was identified as prohibitin (PHB) according to its MALDI-TOF-MS mass spectrum. (D) Protein sequence of PHB is shown and matched peptides are underlined. (E) Western blot analysis of PHB protein levels with PHB/GAPDH ratio as control for the comparison of the grayscale. (F) RT-PCR analysis of PHB mRNA levels. The grayscale ratio of PHB/GAPDH is provided for comparison. $^{*}P<0.05$; $^{**}P<0.01$.

22.16±3.92%, respectively (Fig. 6A). Thus, there was a 2.0-fold less As_4S_4-induced apoptosis in KD than that in parental NB4-R1.

PML-RARα fusion protein of KD cells by western blot analysis. By using the grayscale ratios of PML-RARα/GAPDH, the levels of PML-RARα protein were determined to be 49.78±1.89% in the untreated cells, and 24.21±1.73 and 37.95±7.79% in As_4S_4-treated NB4-R1 and KD cells, respectively. Using the untreated cells as the baseline, As_4S_4 lowered PML-RARα protein by 51.3 and 23.7% in NB4-R1 and KD cells, respectively (Fig. 6B). The results indicate that KD cells presented with a lesser degree of As_4S_4-induced PML-RARα degradation, ~50% of that in parental NB4-R1 cells.

Discussion

Arsenic agents have been proved highly effective in the treatment of APL. It is particularly useful for relapsed/refractory APL with ATRA-resistance (18). As_4S_4, is a new and prom-

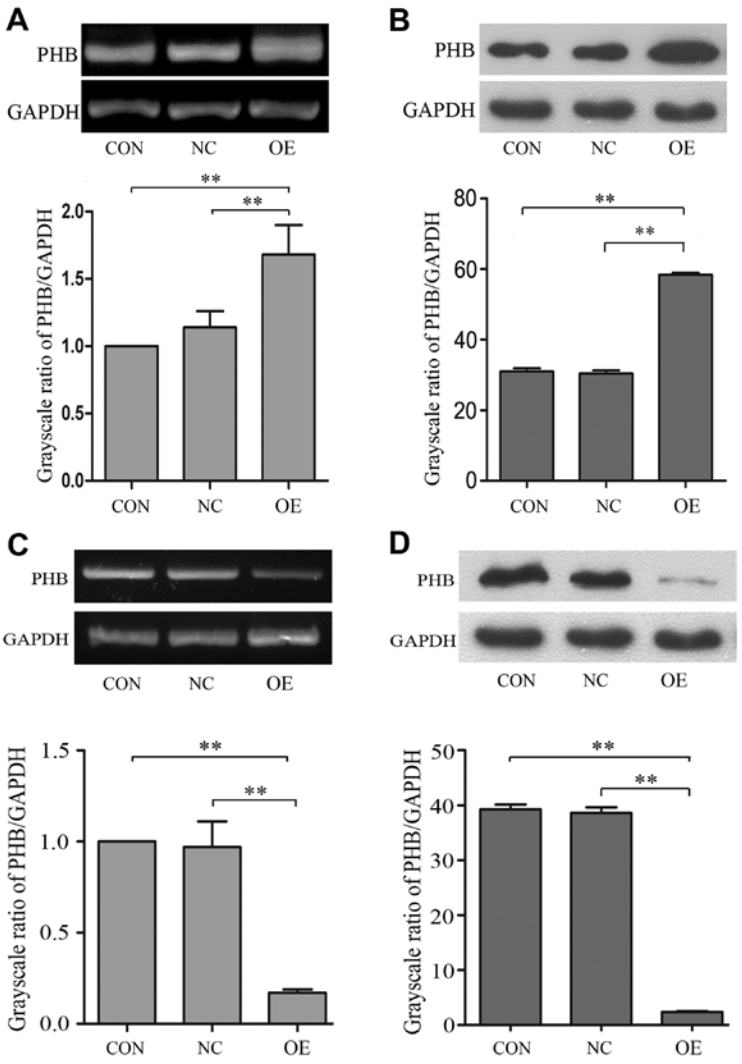

Figure 4. RT-PCR and western blot analysis of PHB overexpression and knockdown in NB4-R1 cells. (A) RT-PCR analysis of PHB overexpression. (B) Western blot analysis of PHB overexpression. (C) RT-PCR analysis of PHB knockdown. (D) Western blot analysis of PHB knockdown. **P<0.01. CON, control (NB4-R1 cells); NC, negative control (NB4-R1 cells transfected with empty vector); KD, PHB-knockdown NB4-R1 cells; OE, PHB-overexpressing NB4-R1 cells.

ising oral arsenic formulation. A multicenter study in China has shown that a complete remission (CR) rate of 99.1% and a disease-free survival (DFS) rate of 98.1% at 2 years were achieved in 108 APL cases treated with an oral As_4S_4 combined with ATRA (19, 20). In the present study, we demonstrated that As_4S_4 inhibited the growth and induced apoptosis of ATRA-resistant NB4-R1 cells. The result is consistent with previous findings (21,22). By using comparative proteomic approach, we identified PHB was significantly upregulated during As_4S_4-induced NB4-R1 apoptosis. As PHB is of particular interest, further experiments were performed to modulate the gene expression, either PHB overexpression or PHB knockdown. The results with modulation of PHB expression implicate its activity in promoting As_4S_4-induced apoptosis.

PHB was selected in this study for its diverse roles in the regulation of proliferation, apoptosis and gene transcription (23-27). PHB proteins have been found to localize in the mitochondria, nucleus and plasma membrane of mammalian cells. PHB is implicated in diverse cellular processes, including mitochondrial biogenesis, cell death and replicative senescence. A functional role for PHB as a regulator of transcription has been shown for its interactions with p53, E2F and Rb (28-30). PHB has been associated with various types of cancer. The role of PHB in cancer cell proliferation or tumor suppression is considered controversial. PHB was shown to be necessary for the activation of C-Raf by the oncogene Ras in HeLa cells (31). However, many reports have shown evidence that PHB has antitumorigenic activity in prostate, gastric and ovarian cancer (32-35). PHB overexpression was shown to result in the inhibition of prostate cancer cell growth and the knockdown of PHB by siRNA accelerates tumor growth (33).

In the present study, stable clones of KD (PHB-knockdown NB4-R1 cells) and OE (PHB-overexpression NB4-R1 cells) were established and used to determine the cellular response to As_4S_4. The results showed that PHB overexpression enhanced apoptosis of NB4-R1 cells, and reduction of PML-RARα fusion protein. Although PHB knockdown had no significant effect on baseline apoptosis and PML-RARα fusion protein, a downregulation of PHB was associated with an attenuated apoptosis and lesser reduction of PML-RARα protein in the cells treated with As_4S_4. These results strongly support that PHB has antitumorigenic activity.

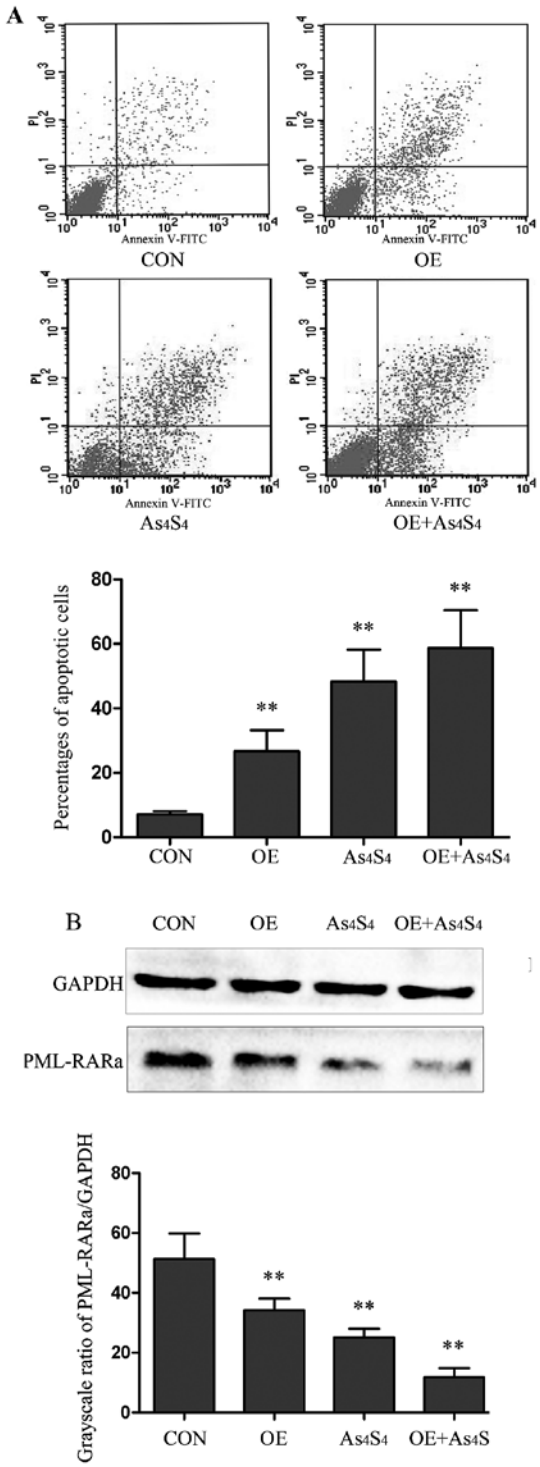

Figure 5. Effect of PHB overexpression on the apoptosis and the expression of PML-RARα protein in NB4-R1 cells induced by As_4S_4. (A) FCM analysis of the apoptosis of the control NB4-R1 cells, OE cells, NB4-R1 cells treated by As_4S_4 and OE cells treated by As_4S_4, respectively. (B) Western blot analysis of the expression of PML-RARα fusion protein. **P<0.01. CON, control (NB4-R1 cells untreated); OE, PHB-overexpression NB4-R1 cells; As_4S_4, NB4-R1 cells treated by As_4S_4; OE+As_4S_4: PHB-overexpressing NB4-R1 cells treated by As_4S_4.

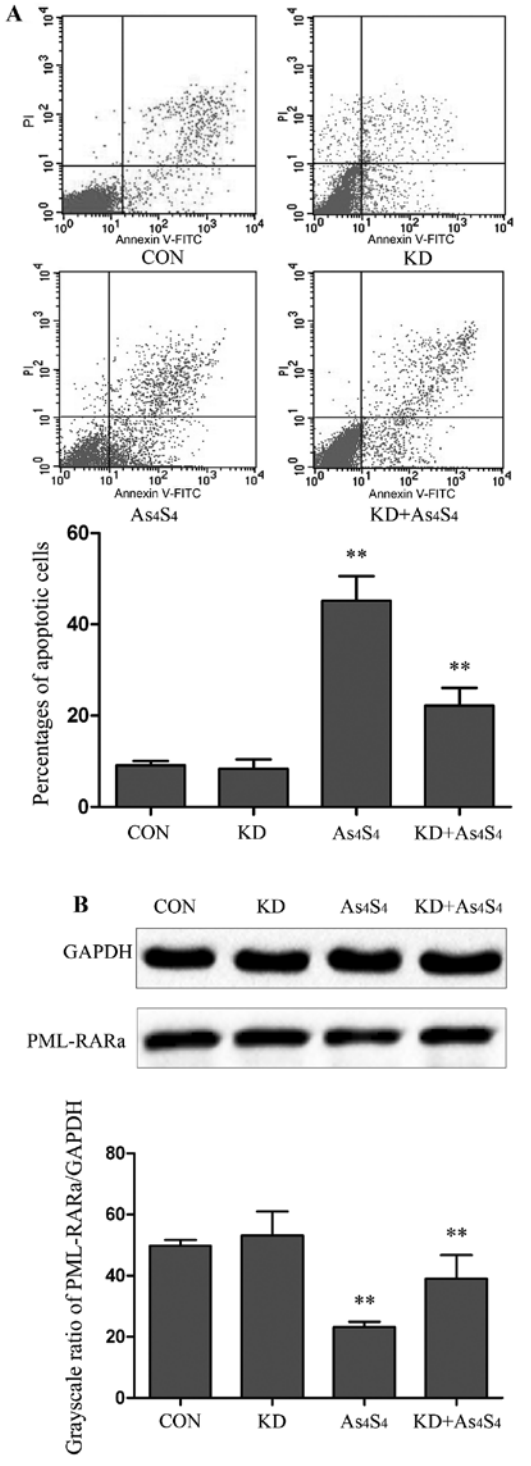

Figure 6. Effect of PHB knockdown on the apoptosis and the expression of PML-RARα protein in NB4-R1 cells induced by As_4S_4. (A) FCM analysis of the apoptosis of NB4-R1 and KD cells untreated, and treated by As_4S_4, respectively. (B) Western blot analysis of the expression of PML-RARα fusion protein. The grayscale ratio of PML-RARα/GAPDH is provided for comparison. **P<0.01. CON, control (NB4-R1 cells untreated); KD, PHB-knockdown NB4-R1 cells; As_4S_4: NB4-R1 cells treated by As_4S_4; KD+As_4S_4: PHB-knockdown NB4-R1 cells treated by As_4S_4.

The effects of PHB on cellular processes may be due to its subcellular localization in different type cells. The subcellular localization of PHB has been shown to affect cell fate, specifically apoptosis (36). PHB has been shown with an increased level on the cell membrane that facilitates tumorigenesis through its interaction with c-Raf induced by the Ras oncogene (37,38), whereas increased levels of PHB in the nucleus induce apoptosis by increasing the transcriptional activity of

p53 and its translocation to the cytoplasm (39). We have found the increased levels of PHB, either modulated by As_4S_4 or by PHB overexpression vectors, in the nucleus locations of APL cells.

The PML-RARα fusion protein is the key molecule that drives APL cells. This fusion protein also serves as the therapeutic target of ATRA and arsenic agents (40). While ATRA induces APL to undergo differentiation by targeting the RARα moiety, arsenic agents induce apoptosis through SUMO-1-mediated degradation of the PML moiety of the fusion protein (41). However, other molecules involved in the process remain to be identified. In this study, we showed a close relationship of upregulation of PHB with reduction of PML-RARα during As_4S_4-induced apoptosis. Consistently, PHB knockdown experiments showed a reduced degradation of PML-RARα protein. These results indicate that PHB is involved in the APL cell apoptosis. However, the biochemical pathway of PHB activity in relation to PML-RARα remains the subject of investigations.

In conclusion, PHB was identified among the upregulated proteins associated with As_4S_4-induced apoptosis of NB4-R1 cells. The experiments with modulation of PHB expression indicate that PHB overexpression enhances apoptosis and degradation of PML-RARα fusion protein, and consistently PHB knockdown attenuated the cellular response to As_4S_4 treatment.

Acknowledgements

The present study is supported by a research grant from the Natural Science Foundation of China (NSFC, grant no. 30701133), the Shaanxi Province Science and Technology Development Fund (SPSTDF, grant no. 2012KTCL03-12). The authors thank Dr Qunling Zhang from Shanghai Institute of Hematology for providing the NB4-R1 cell line; Dr Xinyang Wang from the First Affiliated Hospital, Xi'an Jiaotong University for their technological assistance; and Dr Byron Song from Univerity of Tronto, Ontario, Canada for critically reading the manuscript.

References

1. Sahin U, Lallemand-Breitenbach V and de Thé H: PML nuclear bodies: Regulation, function and therapeutic perspectives. J Pathol 234: 289-291, 2014.
2. Rabellino A, Carter B, Konstantinidou G, Wu SY, Rimessi A, Byers LA, Heymach JV, Girard L, Chiang CM, Teruya-Feldstein J, *et al*: The SUMO E3-ligase PIAS1 regulates the tumor suppressor PML and its oncogenic counterpart PML-RARA. Cancer Res 72: 2275-2284, 2012.
3. Guo Y, Dolinko AV, Chinyengetere F, Stanton B, Bomberger JM, Demidenko E, Zhou DC, Gallagher R, Ma T, Galimberti F, *et al*: Blockade of the ubiquitin protease UBP43 destabilizes transcription factor PML/RARα and inhibits the growth of acute promyelocytic leukemia. Cancer Res 70: 9875-9885, 2010.
4. de Thé H and Chen Z: Acute promyelocytic leukaemia: Novel insights into the mechanisms of cure. Nat Rev Cancer 10: 775-783, 2010.
5. Wang ZY and Chen Z: Acute promyelocytic leukemia: From highly fatal to highly curable. Blood 111: 2505-2515, 2008.
6. Tomita A, Kiyoi H and Naoe T: Mechanisms of action and resistance to all-*trans* retinoic acid (ATRA) and arsenic trioxide (As_2O_3) in acute promyelocytic leukemia. Int J Hematol 97: 717-725, 2013.
7. Mathews V, George B, Lakshmi KM, Viswabandya A, Bajel A, Balasubramanian P, Shaji RV, Srivastava VM, Srivastava A and Chandy M: Single-agent arsenic trioxide in the treatment of newly diagnosed acute promyelocytic leukemia: Durable remissions with minimal toxicity. Blood 107: 2627-2632, 2006.
8. Lengfelder E, Hofmann WK and Nowak D: Impact of arsenic trioxide in the treatment of acute promyelocytic leukemia. Leukemia 26: 433-442, 2012.
9. Wu J, Shao Y, Liu J, Chen G and Ho PC: The medicinal use of realgar (As_4S_4) and its recent development as an anticancer agent. J Ethnopharmacol 135: 595-602, 2011.
10. Lengfelder E, Hofmann WK and Nowak D: Treatment of acute promyelocytic leukemia with arsenic trioxide: Clinical results and open questions. Expert Rev Anticancer Ther 13: 1035-1043, 2013.
11. van Meerloo J, Kaspers GJ and Cloos J: Cell sensitivity assays: the MTT assay. Methods Mol Biol 731: 237-245, 2011.
12. Qian X, Dong H, Hu X, Tian H, Guo L, Shen Q, Gao X and Yao W: Analysis of the interferences in quantitation of a site-specifically PEGylated exendin-4 analog by the Bradford method. Anal Biochem 465: 50-52, 2014.
13. Rabilloud T and Lelong C: Two-dimensional gel electrophoresis in proteomics: A tutorial. J Proteomics 74: 1829-1841, 2011.
14. Dupont FM, Vensel WH, Tanaka CK, Hurkman WJ and Altenbach SB: Deciphering the complexities of the wheat flour proteome using quantitative two-dimensional electrophoresis, three proteases and tandem mass spectrometry. Proteome Sci 9: 10, 2011.
15. Lelong C, Chevallet M, Luche S and Rabilloud T: Silver staining of proteins in 2DE gels. Methods Mol Biol 519: 339-350, 2009.
16. Granvogl B, Plöscher M and Eichacker LA: Sample preparation by in-gel digestion for mass spectrometry-based proteomics. Anal Bioanal Chem 389: 991-1002, 2007.
17. Liu Y, He P, Zhang M and Wu D: Lentiviral vector-mediated RNA interference targeted against prohibitin inhibits apoptosis of the retinoic acid-resistant acute promyelocytic leukemia cell line NB4-R1. Mol Med Rep 6: 1288-1292, 2012.
18. Lu DP, Qiu JY, Jiang B, Wang Q, Liu KY, Liu YR and Chen SS: Tetra-arsenic tetra-sulfide for the treatment of acute promyelocytic leukemia: A pilot report. Blood 99: 3136-3143, 2002.
19. Zhu HH, Wu DP, Jin J, Li JY, Ma J, Wang JX, Jiang H, Chen SJ and Huang XJ: Oral tetra-arsenic tetra-sulfide formula versus intravenous arsenic trioxide as first-line treatment of acute promyelocytic leukemia: A multicenter randomized controlled trial. J Clin Oncol 31: 4215-4221, 2013.
20. Zhu HH and Huang XJ: Oral arsenic and retinoic acid for non-high-risk acute promyelocytic leukemia. N Engl J Med 371: 2239-2241, 2014.
21. Wang L, Zhou GB, Liu P, Song JH, Liang Y, Yan XJ, Xu F, Wang BS, Mao JH, Shen ZX, *et al*: Dissection of mechanisms of Chinese medicinal formula Realgar-*Indigo naturalis* as an effective treatment for promyelocytic leukemia. Proc Natl Acad Sci USA 105: 4826-4831, 2008.
22. Chen S, Fang Y, Ma L, Liu S and Li X: Realgar-induced apoptosis and differentiation in all-trans retinoic acid (ATRA)-sensitive NB4 and ATRA-resistant MR2 cells. Int J Oncol 40: 1089-1096, 2012.
23. Zhou TB and Qin YH: Signaling pathways of prohibitin and its role in diseases. J Recept Signal Transduct Res 33: 28-36, 2013.
24. Rossi L, Bonuccelli L, Iacopetti P, Evangelista M, Ghezzani C, Tana L and Salvetti A: Prohibitin 2 regulates cell proliferation and mitochondrial cristae morphogenesis in planarian stem cells. Stem Cell Rev 10: 871-887, 2014.
25. Liu YH, Peck K and Lin JY: Involvement of prohibitin upregulation in abrin-triggered apoptosis. Evid Based Complement Alternat Med 2012: 605154, 2012.
26. Puppin C, Passon N, Franzoni A, Russo D and Damante G: Histone deacetylase inhibitors control the transcription and alternative splicing of prohibitin in thyroid tumor cells. Oncol Rep 25: 393-397, 2011.
27. Joshi B, Ko D, Ordonez-Ercan D and Chellappan SP: A putative coiled-coil domain of prohibitin is sufficient to repress E2F1-mediated transcription and induce apoptosis. Biochem Biophys Res Commun 312: 459-466, 2003.
28. Chander H, Halpern M, Resnick-Silverman L, Manfredi JJ and Germain D: Skp2B attenuates p53 function by inhibiting prohibitin. EMBO Rep 11: 220-225, 2010.

29. Joshi B, Rastogi S, Morris M, Carastro LM, DeCook C, Seto E and Chellappan SP: Differential regulation of human YY1 and caspase 7 promoters by prohibitin through E2F1 and p53 binding sites. Biochem J 401: 155-166, 2007.
30. Wang S, Fusaro G, Padmanabhan J and Chellappan SP: Prohibitin co-localizes with Rb in the nucleus and recruits N-CoR and HDAC1 for transcriptional repression. Oncogene 21: 8388-8396, 2002.
31. Rajalingam K, Wunder C, Brinkmann V, Churin Y, Hekman M, Sievers C, Rapp UR and Rudel T: Prohibitin is required for Ras-induced Raf-MEK-ERK activation and epithelial cell migration. Nat Cell Biol 7: 837-843, 2005.
32. Wang S and Faller DV: Roles of prohibitin in growth control and tumor suppression in human cancers. Transl Oncogenomics 3: 23-37, 2008.
33. Dart DA, Spencer-Dene B, Gamble SC, Waxman J and Bevan CL: Manipulating prohibitin levels provides evidence for an in vivo role in androgen regulation of prostate tumours. Endocr Relat Cancer 16: 1157-1169, 2009.
34. Zhang Y, Chen Y, Qu C, Zhou M, Ni Q and Xu L: siRNA targeting prohibitins inhibits proliferation and promotes apoptosis of gastric carcinoma cell line SGC7901 in vitro and in vivo. Cell Mol Biol (Noisy-le-grand) 60: 26-32, 2014.
35. Jia L, Ren JM, Wang YY, Zheng Y, Zhang H, Zhang Q, Kong BH and Zheng WX: Inhibitory role of prohibitin in human ovarian epithelial cancer. Int J Clin Exp Pathol 7: 2247-2255, 2014.
36. Theiss AL and Sitaraman SV: The role and therapeutic potential of prohibitin in disease. Biochim Biophys Acta 1813: 1137-1143, 2011.
37. Rajalingam K and Rudel T: Ras-Raf signaling needs prohibitin. Cell Cycle 4: 1503-1505, 2005.
38. Chowdhury I, Thompson WE and Thomas K: Prohibitins role in cellular survival through Ras-Raf-MEK-ERK pathway. J Cell Physiol 229: 998-1004, 2014.
39. Song W, Tian L, Li SS, Shen DY and Chen QX: The aberrant expression and localization of prohibitin during apoptosis of human cholangiocarcinoma Mz-ChA-1 cells. FEBS Lett 588: 422-428, 2014.
40. Zhou GB, Zhang J, Wang ZY, Chen SJ and Chen Z: Treatment of acute promyelocytic leukaemia with all-trans retinoic acid and arsenic trioxide: A paradigm of synergistic molecular targeting therapy. Philos Trans R Soc Lond B Biol Sci 362: 959-971, 2007.
41. Shinagawa K: All-trans retinoic acid and arsenic trioxide: Their molecular mechanisms of action and updated clinical progress in APL therapy. Rinsho Ketsueki 52: 469-483, 2011 (In Japanese).